# Rotationally elastic and inelastic dynamics of NO(X-2 Pi, v=0) in collisions with Ar

# Rotationally elastic and inelastic dynamics of NO(X2, v = 0) in collisions with Ar

G. Paterson, A. Relf, M. L. Costen, K. G. McKendrick, M. H. Alexander, and P. J. Dagdigian

Citation: The Journal of Chemical Physics **135**, 234304 (2011); doi: 10.1063/1.3665135
View online: http://dx.doi.org/10.1063/1.3665135
View Table of Contents: http://scitation.aip.org/content/aip/journal/jcp/135/23?ver=pdfcov
Published by the AIP Publishing

# Rotationally elastic and inelastic dynamics of NO($X^2\Pi$, v = 0) in collisions with Ar

G. Paterson,[1] A. Relf,[1] M. L. Costen,[1] K. G. McKendrick,[1,a)] M. H. Alexander,[2] and P. J. Dagdigian[3,b)]
[1]*School of Engineering and Physical Sciences, Heriot-Watt University, Edinburgh, EH14 4AS, United Kingdom*
[2]*Department of Chemistry and Biochemistry and Institute for Physical Science and Technology, University of Maryland, College Park, Maryland 20742-2021, USA*
[3]*Department of Chemistry, The Johns Hopkins University, Baltimore, Maryland, 21218-2685, USA*

(Received 5 August 2011; accepted 10 November 2011; published online 19 December 2011)

A combined theoretical and experimental study of the depolarization of selected NO($X^2\Pi$, v = 0, $j$, $F$, $\varepsilon$) levels in collisions with a thermal bath of Ar has been carried out. Rate constants for elastic depolarization of rank $K = 1$ (orientation) and $K = 2$ (alignment) were extracted from collision-energy-dependent quantum scattering calculations, along with those for inelastic population transfer to discrete product levels. The rate constants for total loss of polarization of selected initial levels, which are the sum of elastic depolarization and population transfer contributions, were measured using a two-color polarization spectroscopy technique. Theory and experiment agree qualitatively that the rate constants for total loss of polarization decline modestly with $j$, but the absolute values differ by significantly more than the statistical uncertainties in the measurements. The reasons for this discrepancy are as yet unclear. The lack of a significant $K$ dependence in the experimental data is, however, consistent with the theoretical prediction that elastic depolarization makes only a modest contribution to the total loss of polarization. This supports a previous conclusion that elastic depolarization for NO($X^2\Pi$) + Ar is significantly less efficient than for the electronically closely related system OH($X^2\Pi$) + Ar [P. J. Dagdigian and M. H. Alexander, J. Chem. Phys. **130**, 204304 (2009)].
 [doi:10.1063/1.3665135]

## I. INTRODUCTION

Collisions between open-shell diatomic molecules and structureless atomic partners give rise to complex energy transfer (ET) processes which challenge experiment and provide one of the most rigorous tests of high-level *ab initio* potential energy surfaces (PESs).[1–4] Most effort in this area has focused on rotational energy transfer (RET) in $^2\Pi$ + closed-shell-atom systems. The electronic coupling in a $^2\Pi$ diatomic gives rise for every rotational quantum number, $j$, to two spin-orbit (or fine-structure) levels, labeled $F_1$ and $F_2$ for electronic projection quantum numbers, $\Omega = \Lambda \pm \Sigma = 1/2$ and 3/2, respectively. Each of these is, in turn, split into two near-degenerate $\Lambda$-doublet states of parity, $\varepsilon = e$ or $f$. These systems are, therefore, intriguing because these splittings require more than one PES to describe the interaction completely,[5] but nevertheless appealing because they are tractable at an exact quantum mechanical (QM) level of theory. Such problems are practically important because of the role that these transient species play in real-world chemical environments, including combustion, technological plasmas, and the atmosphere. The collision dynamics of NO($X^2\Pi$), which is also the main interest here, has received particular attention.[6] Other prototypical examples include CH($X^2\Pi$),[7–9] OH($X^2\Pi$),[10–14] and CN($A^2\Pi$),[15–23] primarily in collisions with rare gas (Rg) atoms.

The state-of-the-art for this research field lies very much in the domain of measuring and calculating vector properties, as we have highlighted in recent review articles.[24,25] Although vector experiments are technically more challenging, the wealth of additional information they provide over their scalar analogues allows very detailed questions about fundamental molecular interactions to be answered. Consequently, they provide a more rigorous test of the best-available *ab initio* PESs. Perhaps the most commonly measured vector property is the differential cross section (DCS), where the velocity of the scattered molecules is determined, ideally product-state specifically, relative to the initial collision vector. Well-defined laboratory-frame velocities are usually produced by intersecting crossed molecular beams (CMBs). There have been a number of DCS measurements for NO($X^2\Pi$) + Rg systems.[26–34] A sophisticated example is provided by Chandler and co-workers,[35–37] who measured the rotational-polarization-dependent DCS for the rotationally excited products of collisions of NO($X^2\Pi$, v = 0, $j$ = 0.5) with Ar. Essentially, they were able to show that both the plane and sense (clockwise or anticlockwise) of rotation altered as a function of product scattering angle. As we will describe in more detail below, there was very good agreement with QM scattering predictions using the most recent NO($X^2\Pi$)–Ar PES by Alexander.[38] This suggests that the anisotropy of the potential was described well.

Despite CMB experiments providing very detailed information on RET propensities and very powerful tests of

a)Electronic mail: k.g.mckendrick@hw.ac.uk.
b)Electronic mail: pjdagdigian@jhu.edu.

 

the PES anisotropy, they are generally limited to measuring scattering from the lowest rotational levels in the ground vibrational and electronic states. There are only a few limited examples of their use to measure DCSs for vibrationally excited molecules[39] and, very recently, electronically excited species.[40] In addition, CMB experiments are unable to measure *absolute* cross sections or rate constants, which are themselves an important test of *ab initio* PESs and may be particularly critical to the understanding of real-world environments.

An alternative is to use an all-optical approach to measure the evolution of vector properties in a thermal bath of the collision partner. A number of methods of this type have been used to measure the decay of, or inelastic transfer of, polarization of the rotational angular momentum. They include resolution of the polarization of fluorescence emission,[41–43] polarization-sensitive optical-optical double resonance schemes,[23,44–51] Zeeman quantum beat spectroscopy,[52–57] and polarization spectroscopy (PS).[58,59] The Edinburgh-based authors have developed PS for this purpose[12–14,57,60–65] and we apply it to NO($X^2\Pi$) + Ar for the first time here. Such experiments are essentially sensitive to the tilting of the rotational angular momentum vector as a result of collisions with a chosen partner. The obvious advantages over the CMB approach are that a range of initial quantum states can be prepared and probed, and absolute rate constants can be measured. This method therefore complements CMB experiments and provides an additional, discrete test of theoretical predictions.

Previous PS work by the Edinburgh group has focused on the dynamics of OH collisions with Rg atomic partners[12–14,57,62] and simple diatomics, such as $N_2$ and $O_2$.[64] The same basic principles apply here. PS is a third-order nonlinear spectroscopic technique and is a variant of four-wave mixing. A pump laser pulse is used to select preferentially those molecules which have a particular *sense* of rotation (orientation), or alternatively those that are rotating in a particular *plane* (alignment). This is achieved through the choice of circular or linear pump polarization, respectively. A pulsed, linearly polarized probe laser beam crosses the pump beam at a small acute angle. If the sample has rotational anisotropy in a level that is connected to a transition resonant with the probe, then a co-propagating signal beam will be generated. A polarizer crossed with respect to the probe beam polarization is used to isolate the component of the signal beam orthogonal to the probe, and this is guided to a detector. The decay of the PS signal is measured as a function of pump-probe delay. This is repeated at different collision partner number densities, allowing the bimolecular rate constant for the decay of the bulk rotational polarization to be extracted. As described more formally below, these experiments are sensitive to two distinct collisional processes: those which destroy the anisotropic $m$ distribution within level $j$ created by the pump laser (elastic depolarization), and those which remove population from the initially prepared rotational state to all other neighboring states (inelastic population transfer).

The previous PS measurements on OH have stimulated theoretical interest.[12,62,65–69] The field was recently extended by some of the current authors to enable QM scattering calculations of $m$-resolved cross sections and elastic depolarization rate constants for both orientation and alignment.[66–69] In conjunction with previously calculated rate constants for the total removal of population, these provided a prediction of the measured quantities in PS experiments on OH($X^2\Pi$) + Ar (Refs. 66, 68, and 69) and OH($X^2\Pi$) + He.[67] The scattering calculations were in reasonable quantitative agreement with experiment for the higher rotational levels, but for lower rotational levels, where elastic depolarization was predicted to be the dominant collisional process, the discrepancies were larger. Nevertheless, both experiment and theory agreed qualitatively that while elastic depolarization was competitive with RET at low-$j$, its efficiency declined rapidly with increasing $j$, over the range of $j$ investigated.

This theoretical work has already been extended to investigate the efficiency of elastic depolarization for NO($X^2\Pi$) + Ar.[68] The main prediction from the theoretical work so far is that the efficiency of elastic depolarization is very much reduced in comparison to OH($X^2\Pi$) + Ar. The comparison between NO($X^2\Pi$) + Ar and OH($X^2\Pi$) + Ar is interesting because these two systems are similar in some respects, but not in others. They are obviously kinematically distinct. The PESs have comparable well-depths, but differ more subtly in terms of the divergence between their respective pairs of non-degenerate surfaces in nonlinear geometries, as we describe more fully below. A main conclusion from the theoretical work so far is that these electronic factors play an important role in the contrasting efficiencies of elastic depolarization for the two systems.

Our aim here is to use the PS experimental technique to test this theoretical prediction for the first time. To do this effectively, the QM scattering rate constants for elastic depolarization have been evaluated for a range of rotational quantum levels. In our previous theoretical work on NO(X)–Ar,[68] the energy dependence of elastic depolarization cross sections was computed for a smaller set of rotational levels. In addition, the inelastic population transfer rate constants for NO($X^2\Pi$, v = 0, $j$ *e/f*) + Ar have been determined because they are needed for a complete prediction of the PS measurements presented here. These quantities have not been measured, nor (perhaps surprisingly) calculated, for NO($X^2\Pi$, v = 0) + Ar prior to this report, despite their more general importance in a number of gas-phase applications.

## II. METHODOLOGY

### A. Formal kinetic analysis

The formal kinetic analysis of the rate of transfer of rotational polarization, under thermal and isotropic collision environments, has been presented by several authors using a state-multipole treatment.[23,25,66,70] The tensor rate for the transfer of rotational polarization from one unique spectroscopic level to another can be defined in terms of the microscopic rates for its transfer between initial and final levels. The relationship is more often quoted in its inverse form[70,71] but readily

inverted[72] to give

$$\Gamma^{(K)}_{j\to j'} = \sum_{m,m'} (-1)^{j-m-j'-m'}(2K+1) \times \begin{pmatrix} j' & j' & K \\ m' & -m' & 0 \end{pmatrix} \begin{pmatrix} j & j & K \\ m & -m & 0 \end{pmatrix} \Gamma_{jm\to j'm'}. \quad (1)$$

Here, $\Gamma^{(K)}_{j\to j'}$ is a tensor rate of rank $K$ ($K = 0$ for population, $K = 1$ for orientation and $K = 2$ for alignment), the terms in parentheses are 3-$j$ symbols and $\Gamma_{jm\to j'm'}$ is the microscopic rate for transfer between $|jm\rangle$ rotational levels. For notational simplicity, the fine-structure and parity labels of the initial and final levels are not included in Eq. (1) and similarly below, except when specifically required.

Equation (1) can be decomposed into components representing the two distinct types of collisional process identified above: elastic depolarization, in which only $m$ is changed, and inelastic energy transfer, in which $j$ and/or the fine-structure or parity labels are altered. We define the rate of elastic depolarization, $\Gamma^{(K)}_{dep,j}$, and population transfer, $\Gamma_{pop,j}$, via Eqs. (2) and (3), respectively,

$$\Gamma^{(K)}_{dep,j} = \Gamma^{(0)}_{j\to j} - \Gamma^{(K)}_{j\to j}, \quad (2)$$

$$\Gamma_{pop,j} = \sum_{j_x} \Gamma_{j\to j_x}. \quad (3)$$

As expressed in Eq. (2), the rate of elastic depolarization is equal to the rate of all elastic scattering, $\Gamma^{(0)}_{j\to j}$ (i.e., elastic in $j$ and the fine-structure and parity labels) minus the rate for retention of rotational polarization with rank $K$, $\Gamma^{(K)}_{j\to j}$, during elastic collisions.[66] As stated in Eq. (3), the removal of population from an initially prepared level to unobserved levels is simply the sum of all the individual rates for transfer between that initial state, $j$, and all other product rotational states, $j_x$ (where again $x$ is to be interpreted to include a change in any of the fine-structure or parity labels). Since this is independent of tensor rank, i.e., sensitive only to population, we have dropped the superscript ($K$). It follows that the total rate for collisional loss of polarization of rank $K$ of a unique spectroscopic level is the sum of the elastic and inelastic contributions:

$$\Gamma^{(K)}_{tot,j} = \Gamma^{(K)}_{dep,j} + \Gamma_{pop,j}. \quad (4)$$

Experimentally, we measure the rate of decay of the polarization of rank $K$ of a given level in the presence of a chosen collider gas, in this case Ar. As we have discussed previously,[12] for a single collision partner the decay rate is directly proportional to the product of its number density and the corresponding bimolecular rate constant, which we define as $k^{(K)}_{\mathrm{PS},j}$, for total removal of polarization of rank $K$. In practice, there may be other contributions from the (fixed) partial pressure of NO or other, non-collisional losses (primarily fly-out from the probe volume or, particularly if the apparatus is not appropriately shielded,[63] stray magnetic fields). Operationally, the observed decay rate $\Gamma^{(K)}_{\mathrm{PS},j}$ of the PS signal therefore obeys a linear relationship

$$\Gamma^{(K)}_{\mathrm{PS},j} = \Gamma^{(K)}_{int,j} + \Gamma^{(K)}_{tot,j} = \Gamma^{(K)}_{int,j} + k^{(K)}_{\mathrm{PS},j}[\mathrm{Ar}], \quad (5)$$

where $\Gamma^{(K)}_{int,j}$ is the phenomenological $K$-dependent zero-pressure intercept and [Ar] is the Ar number density.

In a similar way, rate constants $k^{(K)}_{dep,j}$ and $k^{(K)}_{pop,j}$ can be defined that correspond to the rates in Eqs. (2) and (3) through multiplication by the collision partner number density. Thus, specifically, the measured PS rate constant, $k^{(K)}_{\mathrm{PS},j}$, can be decomposed, similar to Eq. (4), into contributions from pure elastic depolarization and population removal

$$k^{(K)}_{\mathrm{PS},j} = k^{(K)}_{dep,j} + k_{pop,j}. \quad (6)$$

To aid comparison with some of our previous reports,[12–14,57,62,64] we note that $k^{(K)}_{\mathrm{PS},j}$ corresponds exactly to what we previously denoted either simply $k_{\mathrm{PS}}$ or more recently $k^{(K)}_{\mathrm{PS}}$; $k^{(K)}_{dep,j}$ is equivalent to $k_{\mathrm{DEP}}$ or $k^{(K)}_{\mathrm{DEP}}$; and $k_{pop,j}$ is equal to $k_{\mathrm{POP}}$.

It should be noted that the elastic and inelastic contributions to $k^{(K)}_{\mathrm{PS},j}$ in Eq. (6) cannot be distinguished directly using PS. However, some indication of their relative magnitudes can be inferred without appealing to other sources of information by comparing $k^{(K)}_{\mathrm{PS},j}$ for the loss of orientation ($K = 1$) and alignment ($K = 2$).[12,57] These measures are connected through what must be physically plausible relationships between the underlying propensities for transfer between microscopic $|jm\rangle$ levels. In particular, any difference between $k^{(1)}_{\mathrm{PS},j}$ and $k^{(2)}_{\mathrm{PS},j}$ immediately implies a non-zero contribution from elastic depolarization. Note that the converse is not necessarily true: in the limit, for example, of total scrambling of polarization on every collision, $k^{(1)}_{\mathrm{PS},j}$ and $k^{(2)}_{\mathrm{PS},j}$ would be equal.[49]

For molecules in $\Pi$ electronic states, the population transfer rate constant, $k_{pop,j}$ can be further decomposed into contributions from pure $\Lambda$-doublet transfer (in other words, the $\Delta j = 0$, fine-structure conserving transition), $k_{\Lambda,j}$, and all other rotationally inelastic processes *excluding* $\Lambda$-doublet transfer, $k_{\mathrm{RET},j}$ (in these latter processes either $j$ and/or the fine-structure level change)

$$k_{pop,j} = k_{\Lambda,j} + k_{\mathrm{RET},j}. \quad (7)$$

Computationally, the bimolecular rate constants, including $k^{(K)}_{dep,j}$ and $k_{pop,j}$ (or either of its components) can be determined from the corresponding energy-dependent cross sections, $\sigma$, through[73]

$$k(T) = \langle v\sigma\rangle = \sqrt{\frac{8}{\pi\mu(k_BT)^3}} \int_0^\infty E_c\sigma(E_c)e^{-E_c/k_BT}dE_c, \quad (8)$$

where $v$ is the initial relative velocity, $E_c$ is the corresponding relative translational energy, and $\mu$ is the NO–Ar reduced mass. In the particular case of a state-to-state transition between specified initial and final spectroscopic levels of a $^2\Pi$ electronic state, the explicit expression for the tensor cross

section is[66,71]

$$\sigma^{(K)}_{jF\varepsilon\rightarrow j'F'\varepsilon'} = \frac{\pi}{k^2_{jF\varepsilon}} \sum_{JJ'll'} (2J+1)(2J'+1)(-1)^{l+l'-j-j'+2J} \times \begin{Bmatrix} j & j & K \\ J & J' & l \end{Bmatrix} \begin{Bmatrix} j' & j' & K \\ J & J' & l' \end{Bmatrix} T^J_{jF\varepsilon l, j'F'\varepsilon' l'} \left(T^{J'}_{jF\varepsilon l, j'F'\varepsilon' l'}\right)^* . \quad (9)$$

The rotational levels are specified by the total angular momentum $j$ of the diatom and the fine-structure and parity indices ($F$ and $\varepsilon$, respectively). In Eq. (9), $k_{jF\varepsilon}$ is the wave vector of the initial level, $J$ is the total angular momentum, $l$ is the orbital (end-over-end) angular momentum of the triatomic complex, $\{\dots\}$ is a $6j$ symbol,[74] and the $T$ are $T$-matrix elements, all expressed in a space-fixed frame. It should be noted that when $K = 0$, Eq. (9) yields the integral elastic cross section.

The calculated tensor cross sections can then be averaged over collision energies, as indicated in Eq. (8), and combined appropriately, as implied by Eqs. (2), (3), (6), and (7), to predict rate constants for the processes of interest and to allow comparison with the experimental results.

In the next two subsections, we describe the methods employed to determine the rate constants for depolarization of specific unique levels of NO($X^2\Pi$, v = 0) in collisions with Ar through quantum scattering calculations and PS measurements

### B. Scattering calculations

We have computed energy-dependent integral and tensor cross sections for the collision of NO($X^2\Pi$) with Ar in a QM treatment of the collision dynamics. The interaction of NO($X^2\Pi$) with a spherical partner can be described by two PESs of A′ and A″ symmetry.[5] We employed the unrestricted coupled-cluster with singles, doubles and perturbative treatment of the triples (UCCSD(T)) PESs computed by Alexander.[38] This PES was computed with the NO bond length fixed at the equilibrium value. We discuss below the previous evidence for the accuracy of these PESs in the context of the current results.

Close-coupling scattering calculations were carried out with the HIBRIDON suite of programs,[75] which has recently been extended to include the calculation of tensor cross sections for open-shell molecules.[66] Care was taken to include a sufficient number of both energetically closed channels and partial waves to ensure convergence of the cross sections. It should be noted that the convergence requirements for elastic cross sections are greater than for inelastic cross sections. At the highest energies considered (2000 $cm^{-1}$), the rotational basis included all levels with $j \leq 25.5$, and the scattering calculations included all total angular momenta $J \leq 400.5\,\hbar$.

Energy-dependent elastic depolarization and total inelastic population transfer cross sections have been computed for the $F_1e$ and $F_1f$ fine-structure levels with rotational angular momenta $j = 1.5$ and 2.5–14.5 (every other $j$ for the latter set). These cross sections have been employed [Eq. (8)] to compute 298 K thermal rate constants for these processes. The resulting rate constants are presented in Table I. (The rate constants will also be presented graphically in Sec. IV when computed and measured rate constants are compared.)

TABLE I. Computed RET, Λ-doublet changing, and elastic depolarization rate constants ($T = 298$ K) for collisions of NO($X^2\Pi$, $j$ $F_1e/f$) levels with Ar (in units of $10^{-10}$ $cm^3$ $s^{-1}$). The total inelastic population transfer rate constant, $k_{pop,j}$ can be determined simply *via* Eq. (7).

| j $\varepsilon$ | $k_{\mathrm{RET},j}$ | $k_{\Lambda,j}$ | $k^{(1)}_{dep,j}$ | $k^{(2)}_{dep,j}$ |
|---|---|---|---|---|
| 1.5 *e* | 3.65 | 0.24 | 0.24 | 0.45 |
| 1.5 *f* | 3.68 | 0.23 | 0.23 | 0.44 |
| 2.5 *e* | 3.58 | 0.12 | 0.17 | 0.35 |
| 2.5 *f* | 3.60 | 0.12 | 0.17 | 0.34 |
| 4.5 *e* | 3.25 | 0.14 | 0.12 | 0.26 |
| 4.5 *f* | 3.26 | 0.14 | 0.11 | 0.25 |
| 6.5 *e* | 3.09 | 0.12 | 0.10 | 0.23 |
| 6.5 *f* | 3.12 | 0.12 | 0.09 | 0.22 |
| 8.5 *e* | 3.00 | 0.09 | 0.08 | 0.21 |
| 8.5 *f* | 3.06 | 0.09 | 0.08 | 0.20 |
| 10.5 *e* | 2.91 | 0.07 | 0.07 | 0.19 |
| 10.5 *f* | 3.02 | 0.07 | 0.07 | 0.19 |
| 12.5 *e* | 2.82 | 0.06 | 0.07 | 0.18 |
| 12.5 *f* | 2.95 | 0.06 | 0.07 | 0.17 |
| 14.5 *e* | 2.72 | 0.05 | 0.06 | 0.16 |
| 14.5 *f* | 2.87 | 0.05 | 0.06 | 0.16 |

### C. PS measurements

The experimental approach is very similar in concept to that in our earlier one-color PS[62] and subsequent two-color PS[12,14,57,64] measurements on the OH radical, including precautions needed to eliminate stray magnetic fields from the interaction region of the vacuum chamber.[63] Consequently, we only address the modifications implemented for the two-color PS measurements of NO($X^2\Pi$) + Ar presented here.

Nitric oxide (BOC, 100%) was transferred directly from its cylinder into the vacuum chamber *via* a mass-flow controller (Aera, 10 SCCM) to achieve a partial pressure of ~5 mTorr. A second independent mass-flow controller (MKS, 1000 SCCM) allowed the admission of the Ar collision partner to provide total pressures in the range 5–2000 mTorr.

A "V-shaped" two-color PS spectroscopic scheme[12] was employed to monitor the collisional evolution of NO($X^2\Pi$, v = 0, $j$) rotational polarizations. The pump laser was tuned to a spectroscopic line in the $A^2\Sigma^+$–$X^2\Pi$ (0,0) band (~226 nm) and the probe to a corresponding line in the $A^2\Sigma^+$–$X^2\Pi$ (1,0) band (~214 nm). The fluence of the pump laser beam was ~350 $\mu J\ cm^{-2}$ and the fluence for the probe beam was considerably weaker, $\leq 50\ \mu J\ cm^{-2}$. Preliminary measurements of fluence dependence of the PS signal intensity had established that these were well within the non-saturating, weakly perturbative regime. The time-averaged bandwidth of pump and probe pulses is comparable to the Doppler width of the transitions (FWHM = 0.10 $cm^{-1}$) so there is no significant discrimination of Doppler sub-groups.

The principal advantage of this two-color approach is the restriction of signal to a unique quantum state in NO($X^2\Pi$). Signal generation from NO($A^2\Sigma^+$) would require transfer of

population, *with retention of polarization*, from NO($A^2\Sigma^+$, $v' = 0, j$) to NO($A^2\Sigma^+$, $v' = 1, j$), which is, of course, thermally inaccessible. Both UV laser beams were produced from Nd:YAG (Surelite II-10) pumped dye laser (Sirah, Cobra-stretch) systems with Coumarin 450 and Stilbene 420 laser dyes for the pump and probe, respectively. Selected members of the $P_1(j)$ and $Q_1(j)$ spectroscopic branches were used for the orientation and alignment measurements, respectively: $P_1(j)$ interrogates $F_1e$ levels, while $Q_1(j)$ probes $F_1f$ levels.

A delay/pulse generator (BNC, 565) provided trigger pulses for the two Nd:YAG lasers. The delay between them was varied in a pseudo-random fashion to acquire pump-probe decay traces. The PS signal was detected by a photomultiplier tube (Hamamatsu, R166UH) and captured by a digital oscilloscope (LeCroy, Waverunner 44Xi, 400 MHz, 10GS/s). Five laser shots were averaged for a given pump-probe delay before a subsequent random delay was selected. Each delay was revisited to achieve ~20–30 shots per delay. The pump-probe profiles were fitted using our previously published theoretical treatment for two-color PS.[61]

## III. RESULTS

### A. Scattering calculations

Elastic tensor and depolarization cross sections for ranks $K = 1$ and 2 were computed for collisions of NO($X^2\Pi$, $v = 0$) $F_1e$ and $F_1f$ rotational/fine-structure levels with rotational angular momenta in the range $j = 1.5$–14.5. In addition, integral cross sections for rotationally inelastic transitions out of these levels were computed and summed to yield total population transfer cross sections.

Figure 1 presents computed energy-dependent elastic depolarization cross sections for the NO($X^2\Pi$) $j = 1.5$, 6.5, and 12.5 $F_1e$ rotational/fine-structure levels as a function of the incident relative translational energy in collisions with Ar. Figure 1(a) is for $K = 1$, corresponding to the loss of orientation, while Fig. 1(b) is for $K = 2$, corresponding to the loss of alignment. We see that the cross sections for $K = 2$ are greater than the corresponding ones for $K = 1$, as we had found previously both experimentally and theoretically for the $F_1$ rotational fine-structure levels of OH($X^2\Pi$) in collisions with Ar.[12,66] We have not included the lowest NO($X^2\Pi$) rotational fine-structure level [$j = 0.5$ $F_1e/f$] in Fig. 1 since this level cannot possess alignment. Moreover, in our previous theoretical study of NO($X^2\Pi$)–Ar collisions, we had found that the $K = 1$ elastic depolarization cross sections for this pair of levels are very small.[68]

We also observe in Fig. 1 that the elastic depolarization cross sections are very large at low collision energies and generally decrease monotonically with increasing collision energy. As seen in previous calculations of elastic depolarization cross sections,[66,67] sharp features are superimposed on the smooth variation of the cross sections as a function of the collision energy. These correspond to resonances arising from the presence of quasibound van der Waals levels and shape resonances due to centrifugal barriers, which are often seen in the energy dependence of rotationally inelastic cross sections for scattering of diatomic molecules.[67,76–78] The elastic depolarization cross sections in Fig. 1 also show a decrease in magnitude with increasing $j$, as also seen in other systems.[66–68,79]

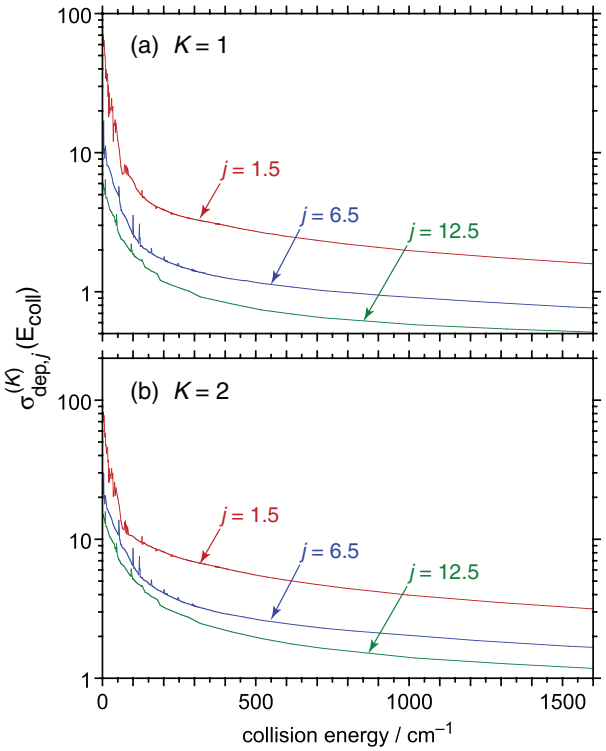


FIG. 1. Computed elastic depolarization cross sections for loss of (a) orientation [$K = 1$] and (b) alignment [$K = 2$] for the NO($X^2\Pi$) $j = 1.5$, 6.5, and 12.5 $F_1e$ rotational/fine-structure levels as a function of the incident relative translational energy in collisions with Ar.

We present in Fig. 2 the energy dependence of the total population transfer cross section, namely, the sum of the cross sections for all rotationally inelastic transitions out of the initial level. We do not discuss the individual state-to-state cross sections since these have been considered in other publications.[38,80–84] As with the elastic depolarization cross sections displayed in Fig. 2, the total inelastic cross sections decrease generally monotonically with increasing collision energy. Sharp features due to resonances are also observed. Comparing the total inelastic cross sections in Fig. 2 and

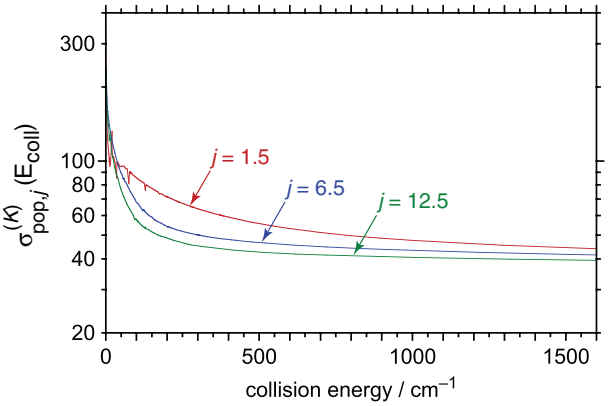


FIG. 2. Computed total population removal cross sections for the NO($X^2\Pi$) $j = 1.5$, 6.5, and 12.5 $F_1e$ rotational/fine-structure levels as a function of the incident relative translational energy in collisions with Ar.

elastic depolarization cross sections in Fig. 1 for the same levels, we see that the inelastic population transfer is substantially more efficient. We also notice that the total inelastic cross sections decrease in size with increasing $j$, but the change with $j$ is smaller than for the elastic depolarization cross sections.

The elastic depolarization rate constants, $k^{(K)}_{dep,j}$, for $K = 1$ and 2, can be seen in Table I to decrease with increasing $j$, as expected from the behavior of the corresponding cross sections plotted in Fig. 1. The rate constants for the $e$ and $f$ levels of a given $j$ are almost identical, with those for the $e$ levels modestly larger in most cases. As noted above for the cross sections, the $K = 2$ rate constants are distinctly larger than their counterparts for $K = 1$.

Similar to the behavior of the corresponding cross sections (see Fig. 2), the total inelastic transfer rate constants can be observed in Table I to decrease with increasing $j$. They are much larger than the rate constants for elastic depolarization. As we have done in our previous work on OH($X^2\Pi$) collisional depolarization,[12,66,67] we consider $\Lambda$-doublet changing collisions as one process contributing to inelastic energy transfer. We see from Table I that the $\Lambda$-doublet changing rate constants are comparable to the rate constants for elastic depolarization.

### B. PS measurements

Examples of PS traces for the decay of orientation and alignment are provided in Fig. 3. The high signal-to-noise ratio achievable using this technique is clearly demonstrated. With close inspection it is possible to observe structure to the fits through the data, more obvious for alignment in Fig. 3(b). These damped oscillations are nuclear hyperfine quantum beats due to the coupling of the nuclear spin of $^{14}$N ($I = 1$) with the rotational angular momentum of NO. This effect is treated fully in the fitting routine. Within the temporal width of our lasers, ~3 ns, the hyperfine levels are excited coherently. Since the hyperfine beats occur on a time scale slower than this (see Table II), they should, in principle, be observable experimentally. However, in practice, for these rotational levels the relatively large $j$:$I$ ratio results in a small amplitude of the oscillatory modulation, which is largely masked by the comparable statistical fluctuations in the experimental PS decay traces.

TABLE II. Nuclear hyperfine frequencies for NO($X^2\Pi_{1/2}$, v = 0, $j$) in units of MHz, calculated using appropriate descriptions for rotational hyperfine matrix elements (Ref. 95) and known spectroscopic constants for NO(X) (Ref. 96). Hyperfine frequencies were calculated for several rotational levels (not quoted here) and compared to measured hyperfine frequencies for NO(X) for verification (Ref. 97).

| j $\varepsilon$ | F = j ← F = j − 1 | F = j + 1 ← F = j |
|---|---|---|
| 6.5 $e$ | 49 | 42 |
| 6.5 $f$ | 72 | 62 |
| 14.5 $e$ | 45 | 40 |
| 14.5 $f$ | 67 | 65 |

A clear empirical observation from Fig. 3 is that the decay of the rotational orientation and alignment for the $j = 6.5$ level shows the expected strong dependence on the partial pressure of Ar. The measured PS decay rate, $\Gamma^{(K)}_{PS,j}$, is plotted against the collision partner number density in Fig. 4. The signal-to-noise level in the decays in Fig. 3 is found to vary partly because a fixed number of laser shots is distributed over a longer interval for the slower decays, but also for purely practical reasons primarily related to the optimization of the optical alignment and the day-to-day stability of the pump and probe pulse energies. We have not found any systematic correlation between this scatter and the deviation from a linear fit to the resulting decay rates in Fig. 4. We therefore use an unbiased least-squares fit to determine the values of the rate

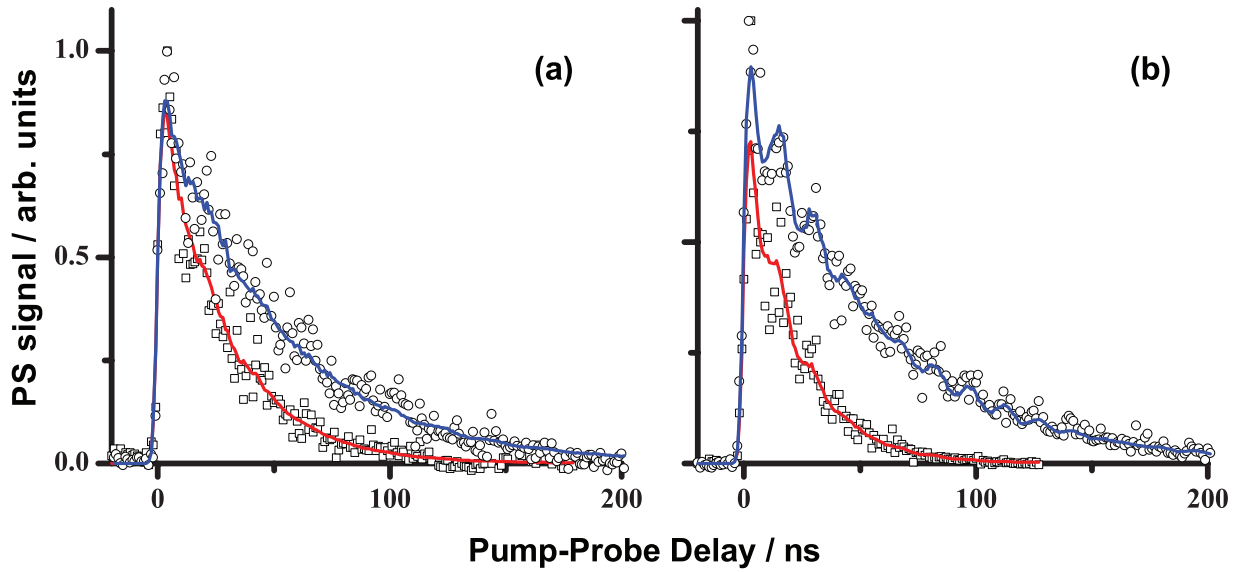


FIG. 3. PS decay traces for NO(X, $j = 6.5$) + Ar collisions for (a) circular pump polarization ($K = 1$) and (b) linear pump polarization ($K = 2$). Selected unique spectroscopic levels ($F_1 f$ and $F_1 e$, respectively) were prepared by pumping on the $Q_1(6.5)$ and $P_1(6.5)$ lines, respectively. Points are the experimental data. Solid lines are fits using the two-color PS theoretical treatment (Ref. 61). The partial pressure of Ar was: in (a) 700 mTorr (circles) and 1300 mTorr (squares); in (b) 540 mTorr (circles) and 1400 mTorr (squares).

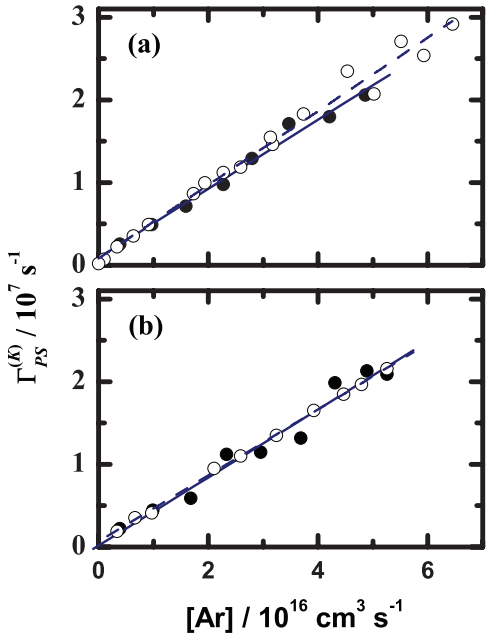


FIG. 4. PS decay rates as a function of Ar number density for (a) $j = 6.5$ and (b) $j = 14.5$. Filled symbols represent orientation ($K = 1$ and hence $e$ levels) and open symbols alignment ($K = 2$ and hence $f$ levels). Lines represent least-square linear fits. Solid lines are associated with $K = 1$ and broken lines with $K = 2$: in (b) the lines are essentially coincident. The slopes yield the bimolecular rate constants, $k_{\mathrm{PS},j}^{(K)}$.

constants and their statistical uncertainties. The resulting phenomenological bimolecular rate constants $k_{\mathrm{PS},j}^{(K)}$ [see Eq. (5)] are collected in Table III.

As an aside, one notable difference between Fig. 3 and equivalent plots for OH($X^2\Pi$),[12,14,64] is the substantial reduction in the observed intercept. For OH($X^2\Pi$) + rare-gases the non-zero intercept was $\sim 5 \times 10^6$ $s^{-1}$, consistent with the partial pressure of $HNO_3$ precursor used and its relatively large rate constant for removal of OH population as measured by Smith and co-workers.[85,86] For the measurements presented here, there is no precursor to NO production, so only "fly-out" and NO self-collisions will contribute to $\Gamma_{int,j}^{(K)}$. Smith and co-workers have also measured RET removal rate constants for NO(X, v = 3, $j$) in self-collisions with NO.[83,84] These rate constants are much lower than for OH + $HNO_3$ collisions, consistent with a much smaller intercept here of roughly $(8 \pm 5) \times 10^5$ $s^{-1}$, to which non-collisional "fly-out" from the volume of the probe laser beam makes a significant contribution.

TABLE III. NO(X) + Ar PS decay rate constants $k_{\mathrm{PS},j}^{(K)}$ (in units of $10^{-10}$ $cm^3$ $s^{-1}$) for loss of orientation ($K = 1$) and of alignment, ($K = 2$) with associated $2\sigma$ statistical uncertainties. Experiments performed at room temperature (nominally 298 K).

| j $\varepsilon$ | $k_{\mathrm{PS},j}^{(1)}$ | $k_{\mathrm{PS},j}^{(2)}$ |
|---|---|---|
| 6.5 $e$ | $4.17 \pm 0.40$ | |
| 6.5 $f$ | | $4.48 \pm 0.28$ |
| 14.5 $e$ | $4.12 \pm 0.60$ | |
| 14.5 $f$ | | $3.93 \pm 0.20$ |

We have also considered but excluded the possibility that the observed decays might be significantly affected by radiative repopulation of the probed level in the NO(X) state. This is primarily a result of the extensive dilution of the emitted population over other rotational and vibrational levels of NO(X), supplemented by efficient collisional depopulation and depolarization of the pumped NO(A) level.[56]

As was apparent from Figs. 2 and 3, and confirmed in Table III, the differences between orientation ($K = 1$) and alignment ($K = 2$) rate constants, $k_{\mathrm{PS},j}^{(K)}$, for a given $j$ are very marginal. For $j = 6.5$, although the values for $K = 1$ and 2 are in the expected order [anticipated from the conclusions of our previous OH($X^2\Pi$) (Refs. 12, 14, 64) and OH($A^2\Sigma^+$) (Ref. 57) studies and from elementary arguments], the difference is barely statistically significant compared to our measurement uncertainty. For $j = 14.5$, the differences are even smaller and, if they were to be significant, the order is actually opposite to that expected physically.

## IV. DISCUSSION

The stated aim of this comparative study is to test the QM scattering prediction that elastic depolarization of NO($X^2\Pi$, v = 0, $j$) in collisions with Ar is considerably less efficient than that for the electronically similar OH($X^2\Pi$). We therefore first concentrate on the differences between the results of QM scattering calculations presented in Sec. III A and the PS experimental measurements presented in Sec. III B.

The final results of the QM scattering calculations are presented graphically alongside the PS measurements in Fig. 5. This plot is constructed such that the total height of the stacked bars is the theoretical prediction of the PS measurements. The bars are decomposed into the collisional processes to whose sum the PS measurements are sensitive: $k_{\mathrm{RET},j}$, $k_{\Lambda,j}$, and $k_{dep,j}^{(K)}$. All these components decline in magnitude as $j$ increases, contributing to the overall $j$-dependent decline predicted for $k_{\mathrm{PS},j}^{(K)}$. Also plotted in Fig. 5 are the PS measurements with their associated 95% confidence limits. Qualitatively, the measurements reflect the predicted mildly downward trend with increasing $j$, but it is quite clear that the QM calculations under-predict the absolute magnitude of the $k_{\mathrm{PS},j}^{(K)}$ measurements. This discrepancy ranges from ~25% to 45%, generally increasing in relative terms with $j$. This was larger than expected, so we have sought above to eliminate possible sources of error. We now consider carefully what more fundamental reasons there might be for the level of disagreement.

The only collisional process that depends on $K$ is elastic depolarization. This is shown explicitly in Table I, where the calculated $k_{dep,j}^{(2)}$ values are approximately a factor of two greater than $k_{dep,j}^{(1)}$. Consequently, an experiment sensitive to elastic depolarization should, in principle, observe this as an equivalent absolute difference between $k_{\mathrm{PS},j}^{(1)}$ and $k_{\mathrm{PS},j}^{(2)}$. Indeed, we have demonstrated exactly this behavior in our previous PS measurements on OH($X^2\Pi$) (Ref. 12) and OH($A^2\Sigma^+$) (Ref. 57) in collisions with rare gases.

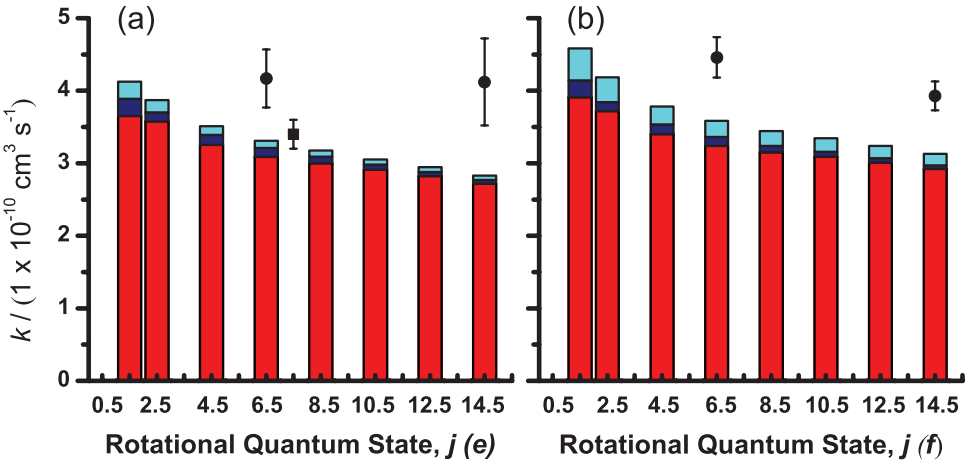


FIG. 5. Thermal (298 K) rate constants for NO(X, v = 0, $F_1 j$). (a) $K = 1$ (orientation) and (b) $K = 2$ (alignment). Rate constants computed by quantum scattering calculations are shown for $k_{\mathrm{RET},j}$ (red), $k_{\Lambda,j}$ (navy) (the sum of which is equal to $k_{pop,j}$) and $k^{(K)}_{dep,j}$ (cyan). The total height of the colored bars therefore represents a calculation of $k^{(K)}_{\mathrm{PS},j}$. Measured $k^{(K)}_{\mathrm{PS},j}$ values are shown (filled circles) with their corresponding statistical uncertainties. An independent measurement of $k_{\mathrm{RET},7.5e}$ (Refs. 83 and 84) is also shown for NO(X, v = 2) (squares).

However, in practice here (see Table III and Fig. 4) the experimental differences between $k^{(2)}_{\mathrm{PS},j}$ and $k^{(1)}_{\mathrm{PS},j}$ are marginal, at most, relative to their uncertainties. The theoretically predicted absolute differences (see Table I) for $j = 6.5$ and 14.5 are around 1.3 and 1.0 × $10^{-11}$ cm$^3$ s$^{-1}$, respectively. These fall well within the uncertainties in the experimental data, which span 2–6 × $10^{-11}$ cm$^3$ s$^{-1}$. The most that can be concluded is therefore that the experiments confirm that the true differences are relatively small. There is actually a subtle complication here in that the experimental values for $k^{(1)}_{\mathrm{PS},j}$ and $k^{(2)}_{\mathrm{PS},j}$ were measured for two different parity levels of the same rotational quantum number, as mentioned in Sec. II B. However, theory suggests that differences in total loss between *e* and *f* levels are also modest, so this does not alter the basic conclusion that any differences in the elastic depolarization contributions must be below the experimental precision.

The lack of any discernible experimental *K*-dependence is therefore also at least consistent with the theoretical prediction that the elastic depolarization is a relatively minor contribution to the overall destruction of polarization. Hence, we conclude that experiment supports, as we report for the first time here, the previous theoretical prediction[68] that the absolute values of elastic depolarization rate constants are much smaller for NO($A^2\Sigma^+$) + Ar than for OH($A^2\Sigma^+$) + Ar.

Since it appears that the dominant contribution to $k^{(K)}_{\mathrm{PS},j}$ is the inelastic contribution, $k_{pop,j}$, it is also likely to be the major source of the discrepancy between experiment and theory. To our knowledge, the only independent absolute experimental measurements of $k_{\mathrm{RET},j}$, which match the conditions and range of *j* investigated here, were carried out by Smith and co-workers.[83,84] They used an optical-optical double resonance technique to obtain state-to-state RET rate constants [excluding Λ-doublet transfer – see Eq. (7)] for a number of product rotational levels from NO($X^2\Pi$, v = 2, $j = 7.5$ *e*) in collisions with Ar. The sum of the rate constants of the individual transitions is equal to $k_{\mathrm{RET},7.5e}$ and was found to be (3.4 ± 0.2) × $10^{-10}$ cm$^3$ s$^{-1}$.

This result has been included in Fig. 5(a) (solid square), but the reader should note that a direct comparison ignores the possible effects of the differences in vibrational level. Smith's value lies somewhat below the adjacent experimental $k^{(1)}_{\mathrm{PS},j}$ values from the present work. This might be expected since the experimental values of Smith and coworkers do not include contributions from $k^{(1)}_{dep,j}$ and $k_{\Lambda,j}$. There have been no prior measurements of state-to-state Λ-doublet transfer for NO($X^2\Pi$) + Ar. Our calculations predict modest values for $k_{\Lambda,j}$ . The interpolated sum of the theoretically predicted $k^{(1)}_{dep,j}$ and $k_{\Lambda,j}$ for $j = 7.5$ *e* is ~0.2 × $10^{-10}$ cm$^3$ s$^{-1}$. Adding this to Smith's value predicts $k^{(1)}_{\mathrm{PS},j}$ to be ~3.6 × $10^{-10}$ cm$^3$ s$^{-1}$. This is significantly smaller than our measurement of (4.2 ± 0.2) × $10^{-10}$ cm$^3$ s$^{-1}$ for $j = 6.5$ *e* (Table III). Also, regardless of the values of $k^{(1)}_{dep,j}$ and $k_{\Lambda,j}$, Smith's value for $k_{\mathrm{RET},7.5e}$ lies significantly above any reasonable interpolation of our theoretically predicted values $k_{\mathrm{RET},j}$ shown by the red bars in Fig. 5.

The discrepancy between theory and experiment could be due to undetected systematic errors in the experiment and/or inadequacies in the treatment of the collision dynamics or in the calculated NO($X^2\Pi$)–Ar PESs. The close-coupling scattering calculations represent an essentially exact treatment of the dynamics.

The PESs were computed at the UCCSD(T) level theory, with the assumption of an internuclear NO separation fixed at $r_e$. This set of PESs has been extensively tested by comparison with experimental measurements of both relative integral and differential state-to-state cross sections. Initial comparisons[38] focused on state-to-state relative integral cross sections out of the lowest Λ-doublet pair ($j = 0.5$ $F_1 e/f$) (Refs. 80 and 82) and out of the upper Λ-doublet ($j = 0.5$ $F_1 f$).[81] Good agreement was found for the variation with *j* of the fine-structure conserving transitions. However, the calculations significantly

underestimated cross sections for fine-structure changing transitions.

As suggested in the Introduction, a more sensitive test of the accuracy of the PESs is provided by differential cross sections. Kohguchi *et al.*[32] measured fully state-resolved differential cross sections for the scattering of NO($X^2\Pi$, $j = 0.5$ $F_1e/f$) by Ar in an ion-imaging experiment. These experimental measurements were compared with calculations using the current PESs and an earlier correlated electron-pair approximation set[87] of PESs. Very good agreement between experiment and theory was found for fine-structure conserving transitions, although, here too, some discrepancies were found for fine-structure changing transitions. Later, Elioff and Chandler[33] re-examined fine-structure changing collisions with a more precise measurement of the scattering in the forward direction. Very good agreement with theory was then found for the differential cross sections for the fine-structure changing collisions. The current PESs also provided a good representation of the preferred sense of NO rotation after collision with Ar, measured in an ion imaging experiment by Lorenz *et al.*[36] Most recently, Brouard *et al.*[4] found excellent agreement between DCS measurements and theoretical predictions based on the Alexander PESs for spin-orbit conserving transitions out of a single Λ-doublet level.

These observations, therefore, suggest that the PESs used here provide an accurate description of the anisotropy of the interaction; however, since they are all relative measurements, they do not necessarily test its absolute range. An independent test of at least the attractive part of the PESs is provided by the bound-state energies of the Ar–NO van der Waals complex. Alexander found that the energies of the rotational levels of the lowest Ar–NO bend-stretch states predicted from these PESs were in generally excellent agreement with those measured by Mills *et al.*[88] through microwave and RF spectroscopy.[89] Meyer and co-workers[90,91] recorded the spectrum of the v = 2 ← v = 0 transition of the Ar–NO complex at high resolution. The observed bands could be assigned with bound-state energies computed with the Alexander PESs. The overall good agreement with Meyer's measurements suggests that this set of PESs provides a good description of at least the attractive part of the interaction. In particular, the agreement with the rotational structure implies that the range of the potential is well predicted.

We note that the present study would not be the first example of a discrepancy between QM scattering calculations and PS measurements. In our previous studies of collisions of OH($X^2\Pi$) with He and Ar, we demonstrated that the PESs calculated by Paterson *et al.* also failed to reproduce exactly the PS measurements.[12,65] In contrast with the present study, in the work of Paterson *et al.* the calculated $k_{pop,j}$ values, and indeed $k^{(K)}_{dep,j}$ are *larger* than seen experimentally.

Despite the commonly held picture that the repulsive wall dominates RET, it is clear from the strong negative energy dependence of inelastic population transfer shown in Fig. 2 that the attractive part of the potential is important. This, therefore, makes it difficult to use simple hard-shell collision models to predict quantitatively the magnitude of RET cross sections in NO($X^2\Pi$)–Ar collisions. We see in Fig. 1 that the elastic depolarization cross sections also decrease strongly with increasing collision energy. The role of attractive forces in elastic depolarization has been inferred from previous PS measurements[12–14,57,62] on OH and demonstrated through calculated collision-energy-dependent cross sections[66,68,69] similar to those shown here for NO($X^2\Pi$)–Ar. Consequently, errors in either the attractive or repulsive regions of PESs could be responsible for the discrepancy with experiment seen in the present work.

We return now to the broader observation that elastic depolarization of NO ($X^2\Pi$) in collisions with Ar is less efficient than that of OH($X^2\Pi$). This was previously predicted[68] and now at least indirectly confirmed here experimentally. The systems both show a fairly rapid decline in the relative $\sigma^{(K)}_{dep,j}$ values as a function of rotational quantum number. This can perhaps be anticipated from elementary classical mechanics: a faster rotating object is more resistant to tilting.

The major difference between NO($X^2\Pi$) and OH($X^2\Pi$) in collisions with Ar is the magnitude of the elastic depolarization cross sections. For NO($X^2\Pi$) + Ar, the low $j$ ($j = 1.5$) value of $\sigma^{(2)}_{dep,j} \approx 8$ Å$^2$ is more than a factor of two smaller than the corresponding result for OH($X^2\Pi$)–Ar of $\sigma^{(2)}_{dep,j} \approx 20$ Å$^2$ inferred from our previous work (both PS measurements and QM scattering calculations).[12] Dagdigian and Alexander attributed this difference to a larger magnitude of the half-difference potential, $V_{\rm diff}$, for the OH–Ar system over the range of impact parameters which make the strongest contribution to rotational inelasticity.[68] To make this conclusion they artificially removed $V_{\rm diff}$. This significantly affected elastic depolarization for OH($X^2\Pi$) + Ar but not for NO($X^2\Pi$) + Ar. (We note in passing that the signs of the coefficients $V_{32}$ and $V_{42}$ that contribute to the radial expansion of $V_{\rm diff}$ are shown correctly as positive in Ref. 68. The apparent discrepancy with earlier work[92] is due to an error in the construction of Fig. 2, but not the underlying PES, in Ref. 92.)

There are a few more differences between the OH($X^2\Pi$) + Ar and NO($X^2\Pi$) + Ar systems whose possible influence on the efficiency of elastic depolarization is yet to be established. Although the depths of the global minima on the two sets of PESs are relatively similar, the geometry of the minimum for OH($X^2\Pi$)–Ar is linear, but T-shaped for NO($X^2\Pi$)–Ar. To judge from earlier work by Mayne and Kiel,[93] based on classical trajectory calculations on model PESs, such differences in the topography of the PES may affect the collision dynamics and, by extension, elastic depolarization.

Of course, NO($X^2\Pi$)–Ar and OH($X^2\Pi$)–Ar also have very different kinematics, most notably because of the difference in moment of inertia of the diatomic rotor and, more weakly, in the reduced mass of the collision pair. The majority of previous studies of kinematic effects have concentrated on the latter type of difference, although for real systems this inevitably involves simultaneous changes in the PESs. For OH($X^2\Pi$) colliding with He and Ar, Esposti *et al.* concluded,[94] after detailed inspection of the PESs, that differences in both the PESs and the reduced mass affect the inelastic cross sections. There is as yet little known about how kinematics influences elastic depolarization. Further work is

needed in this area to disentangle PES and kinematic effects. In particular, investigation (both experimental and theoretical) of the NO($X^2\Pi$)+He system would provide an invaluable mass-dependent comparison for collisions of NO.

## V. CONCLUSIONS

We have presented here a detailed comparison between PS measurements and high-level quantum scattering calculations of the molecular collision dynamics of NO($X^2\Pi$) + Ar. Rate constants for inelastic population transfer and elastic depolarization have been calculated for a number of rotational levels and combined to provide a prediction of the PS measurements of overall collisional destruction of polarization. Overall, experiment and theory are in qualitative agreement on a modest decline in the rate constant for total loss of polarization with increasing $j$. However, the values predicted theoretically are 25%–45% lower than those that are measured. Since both measurements and theory are consistent with elastic depolarization making a minor contribution to this total loss, the discrepancy presumably must lie in the comparison of calculated and measured rate constants for inelastic population transfer.

The PS measurements support the previous prediction,[68] and the more detailed calculations presented here, that elastic depolarization for NO($X^2\Pi$) + Ar is substantially less efficient than in the well studied OH($X^2\Pi$) + Ar system, also involving a molecule in a $^2\Pi$ electronic state. Differences in the PESs, and in particular the difference potentials, $V_{\text{diff}}$, have already been shown to contribute to this observation. In addition, differences in kinematics may also play a significant role.

## ACKNOWLEDGMENTS

We thank Rebecca Sure and Franziska Hegner for their contributions to the early development of the PS work. We acknowledge a grant from EPSRC to support the experimental part of this work and a grant from the U.S. National Science Foundation (Grant No. CHE-0848110) to support the theoretical portion.

[1] P. J. Dagdigian, in *The Chemical Dynamics and Kinetics of Small Free Radicals, Part I*, edited by K. Liu and A. Wagner (World Science, Singapore, 1995), p. 315.
[2] P. J. Dagdigian, Annu. Rev. Phys. Chem. **48**, 95 (1997).
[3] A. Schiffman and D. W. Chandler, Int. Rev. Phys. Chem. **14**, 371 (1995).
[4] C. J. Eyles, M. Brouard, C.-H. Yang, J. Klos, F. J. Aoiz, A. Gijsbertsen, A. E. Wiskerke, and S. Stolte, Nat. Chem. **3**, 597 (2011).
[5] M. H. Alexander, Chem. Phys. **92**, 337 (1985).
[6] D. W. Chandler and S. Stolte, in *Gas Phase Reaction and Photodissociation Dynamics*, edited by K. C. Lin and P. D. Kleiber (Transworld Research Network, Kerala, India, 2007), p. 1.
[7] S. M. Ball, G. Hancock, and M. R. Heal, J. Chem. Soc., Faraday Trans. **90**, 1467 (1994).
[8] M. H. Alexander and P. J. Dagdigian, J. Chem. Phys. **101**, 7468 (1994).
[9] P. Heinrich and F. Stuhl, J. Chem. Phys. **102**, 618 (1995).
[10] M. C. van Beek, J. J. ter Meulen, and M. H. Alexander, J. Chem. Phys. **113**, 628 (2000).
[11] M. C. van Beek, J. J. ter Meulen, and M. H. Alexander, J. Chem. Phys. **113**, 637 (2000).
[12] G. Paterson, S. Marinakis, M. L. Costen, K. G. McKendrick, J. Klos, and R. Tobola, J. Chem. Phys. **129**, 074304 (2008).
[13] G. Paterson, S. Marinakis, M. L. Costen, and K. G. McKendrick, Phys. Scr. **80**, 048111 (2009).
[14] G. Paterson, S. Marinakis, J. Klos, M. L. Costen, and K. G. McKendrick, Phys. Chem. Chem. Phys. **11**, 8804 (2009).
[15] X. Yang and P. J. Dagdigian, Chem. Phys. Lett. **297**, 506 (1998).
[16] M. H. Alexander, X. Yang, P. J. Dagdigian, A. Berning, and H. J. Werner, J. Chem. Phys. **112**, 781 (2000).
[17] X. Yang, P. J. Dagdigian, and M. H. Alexander, J. Chem. Phys. **112**, 4474 (2000).
[18] B. Nizamov, P. J. Dagdigian, and M. H. Alexander, J. Chem. Phys. **115**, 8393 (2001).
[19] B. Nizamov, P. J. Dagdigian, Y. R. Tzeng, and M. H. Alexander, J. Chem. Phys. **115**, 800 (2001).
[20] B. Nizamov, X. Yang, P. J. Dagdigian, and M. H. Alexander, J. Phys. Chem. A **106**, 8345 (2002).
[21] A. Alagappan, I. Ballingall, M. L. Costen, and K. G. McKendrick, J. Chem. Phys. **126**, 041103 (2007).
[22] A. Alagappan, I. Ballingall, M. L. Costen, K. G. McKendrick, and G. Paterson, Phys. Chem. Chem. Phys. **9**, 747 (2007).
[23] I. Ballingall, M. F. Rutherford, K. G. McKendrick, and M. L. Costen, Mol. Phys. **108**, 847 (2010).
[24] M. L. Costen, S. Marinakis, and K. G. McKendrick, Chem. Soc. Rev. **37**, 732 (2008).
[25] G. Paterson, M. L. Costen, and K. G. McKendrick, Mol. Phys. **109**, 2565 (2011).
[26] A. A. Dixit, P. J. Pisano, and P. L. Houston, J. Phys. Chem. A **105**, 11165 (2001).
[27] M. S. Westley, K. T. Lorenz, D. W. Chandler, and P. L. Houston, J. Chem. Phys. **114**, 2669 (2001).
[28] S. D. Jons, J. E. Shirley, M. T. Vonk, C. F. Giese, and W. R. Gentry, J. Chem. Phys. **97**, 7831 (1992).
[29] S. D. Jons, J. E. Shirley, M. T. Vonk, C. F. Giese, and W. R. Gentry, J. Chem. Phys. **105**, 5397 (1996).
[30] A. G. Suits, L. S. Bontuyan, P. L. Houston, and B. J. Whitaker, J. Chem. Phys. **96**, 8618 (1992).
[31] L. S. Bontuyan, A. G. Suits, P. L. Houston, and B. J. Whitaker, J. Phys. Chem. **97**, 6342 (1993).
[32] H. Kohguchi, T. Suzuki, and M. H. Alexander, Science **294**, 832 (2001).
[33] M. S. Elioff and D. W. Chandler, J. Chem. Phys. **117**, 6455 (2002).
[34] A. Gijsbertsen, H. Linnartz, G. Rus, A. E. Wiskerke, S. Stolte, D. W. Chandler, and J. Klos, J. Chem. Phys. **123**, 224305 (2005).
[35] J. I. Cline, K. T. Lorenz, E. A. Wade, J. W. Barr, and D. W. Chandler, J. Chem. Phys. **115**, 6277 (2001).
[36] K. T. Lorenz, D. W. Chandler, J. W. Barr, W. W. Chen, G. L. Barnes, and J. I. Cline, Science **293**, 2063 (2001).
[37] E. A. Wade, K. T. Lorenz, D. W. Chandler, J. W. Barr, G. L. Barnes, and J. I. Cline, Chem. Phys. **301**, 261 (2004).
[38] M. H. Alexander, J. Chem. Phys. **111**, 7426 (1999).
[39] M. Drabbels, A. M. Wodtke, M. Yang, and M. H. Alexander, J. Phys. Chem. A **101**, 6463 (1997).
[40] J. J. Kay, G. Paterson, M. L. Costen, K. E. Strecker, K. G. McKendrick, and D. W. Chandler, J. Chem. Phys. **134**, 091101 (2011).
[41] A. J. McCaffery, M. J. Proctor, and B. J. Whitaker, Annu. Rev. Phys. Chem. **37**, 223 (1986).
[42] N. A. Jackson, C. J. Randall, and K. G. McKendrick, Chem. Phys. **233**, 45 (1998).
[43] K. G. McKendrick, J. Chem. Soc., Faraday Trans. **94**, 1921 (1998).
[44] L. D. Snow, R. N. Compton, and J. C. Miller, J. Chem. Phys. **88**, 1652 (1988).
[45] J. B. Halpern, R. Dopheide, and H. Zacharias, J. Phys. Chem. **99**, 13611 (1995).
[46] J. B. Halpern, R. Dopheide, and H. Zacharias, Astrophys. Space Sci. **236**, 19 (1996).
[47] T. G. A. Heijmen, R. Moszynski, P. E. S. Wormer, A. van der Avoird, A. D. Rudert, J. B. Halpern, J. Martin, W. B. Gao, and H. Zacharias, J. Chem. Phys. **111**, 2519 (1999).
[48] A. D. Rudert, J. Martin, W. B. Gao, J. B. Halpern, and H. Zacharias, J. Chem. Phys. **111**, 9549 (1999).
[49] A. D. Rudert, J. Martin, W. B. Gao, H. Zacharias, and J. B. Halpern, J. Chem. Phys. **112**, 9749 (2000).
[50] S. J. Silvers, R. A. Gottscho, and R. W. Field, J. Chem. Phys. **74**, 6000 (1981).
[51] J. B. Norman and R. W. Field, J. Chem. Phys. **92**, 76 (1990).

[52]M. Brouard, A. Bryant, I. Burak, S. Marinakis, F. Quadrini, I. A. Garcia, and C. Vallance, Mol. Phys. **103**, 1693 (2005).
[53]F. J. Aoiz, M. Brouard, C. J. Eyles, J. Kłos, and M. P. D. Miranda, J. Chem. Phys. **130**, 044305 (2009).
[54]M. Brouard, A. Bryant, Y. P. Chang, R. Cireasa, C. J. Eyles, A. M. Green, S. Marinakis, F. J. Aoiz, and J. Kłos, J. Chem. Phys. **130**, 044306 (2009).
[55]M. Brouard, H. Chadwick, Y. P. Chang, R. Cireasa, and C. J. Eyles, Phys. Scr. **80**, 048120 (2009).
[56]M. Brouard, H. Chadwick, Y. P. Chang, R. Cireasa, C. J. Eyles, A. O. La Via, N. Screen, F. J. Aoiz, and J. Klos, J. Chem. Phys. **131**, 104307 (2009).
[57]M. L. Costen, R. Livingstone, K. G. McKendrick, G. Paterson, M. Brouard, H. Chadwick, Y. P. Chang, C. J. Eyles, F. J. Aoiz, and J. Klos, J. Phys. Chem. A **113**, 15156 (2009).
[58]X. L. Chen, B. D. Patterson, and T. B. Settersten, Chem. Phys. Lett. **388**, 358 (2004).
[59]R. Tadday, A. Dreizler, A. A. Suvernev, and T. Dreier, J. Mol. Struct. **410-411**, 85 (1997).
[60]M. L. Costen, H. J. Crichton, and K. G. McKendrick, J. Chem. Phys. **120**, 7910 (2004).
[61]M. L. Costen and K. G. McKendrick, J. Chem. Phys. **122**, 164309 (2005).
[62]S. Marinakis, G. Paterson, J. Klos, M. L. Costen, and K. G. McKendrick, Phys. Chem. Chem. Phys. **9**, 4414 (2007).
[63]S. Marinakis, G. Paterson, G. Richmond, M. Rockingham, M. L. Costen, and K. G. McKendrick, J. Chem. Phys. **128**, 021101 (2008).
[64]G. Paterson, S. Marinakis, M. L. Costen, and K. G. McKendrick, Phys. Chem. Chem. Phys. **11**, 8813 (2009).
[65]G. Paterson, S. Marinakis, M. L. Costen, K. G. McKendrick, J. Klos, and R. Tobola, J. Chem. Phys. **131**, 159901 (2009).
[66]P. J. Dagdigian and M. H. Alexander, J. Chem. Phys. **130**, 094303 (2009).
[67]P. J. Dagdigian and M. H. Alexander, J. Chem. Phys. **130**, 164315 (2009).
[68]P. J. Dagdigian and M. H. Alexander, J. Chem. Phys. **130**, 204304 (2009).
[69]P. J. Dagdigian and M. H. Alexander, J. Chem. Phys. **131**, 229902 (2009).
[70]B. Follmeg, P. Rosmus, and H. J. Werner, J. Chem. Phys. **93**, 4687 (1990).
[71]M. H. Alexander and S. L. Davis, J. Chem. Phys. **78**, 6754 (1983).
[72]M. Brouard, personal communication (2008).
[73]I. W. M. Smith, *Kinetics and Dynamics of Elementary Gas Reactions* (Butersworths, London, 1980).
[74]R. N. Zare, *Angular Momentum: Understanding Spatial Aspects in Chemistry and Physics* (Wiley, New York, 1988).
[75]E. W. Wilson, Jr., W. A. Hamilton, H. R. Kennington, B. Evans III, N. W. Scott, and W. B. DeMore, J. Phys. Chem. A **110**, 3593 (2006).
[76]L. N. Smith, D. J. Malik, and D. Secrest, J. Chem. Phys. **71**, 4502 (1979).
[77]K. M. Christoffel and J. M. Bowman, J. Chem. Phys. **78**, 3952 (1983).
[78]F. Lique, A. Spielfiedel, N. Feautrier, I. F. Schneider, J. Klos, and M. H. Alexander, J. Chem. Phys. **132**, 024303 (2010).
[79]P. J. Dagdigian and M. Alexander, Mol. Phys. **108**, 1159 (2010).
[80]H. Joswig, P. Andresen, and R. Schinke, J. Chem. Phys. **85**, 1904 (1986).
[81]J. J. van Leuken, F. H. W. Vanamerom, J. Bulthuis, J. G. Snijders, and S. Stolte, J. Phys. Chem. **99**, 15573 (1995).
[82]A. Lin, S. Antonova, A. P. Tsakotellis, and G. C. McBane, J. Phys. Chem. A **103**, 1198 (1999).
[83]M. Islam, I. W. M. Smith, and M. H. Alexander, Chem. Phys. Lett. **305**, 311 (1999).
[84]M. Islam, I. W. M. Smith, and M. H. Alexander, Phys. Chem. Chem. Phys. **2**, 473 (2000).
[85]K. M. Hickson, C. M. Sadowski, and I. W. M. Smith, Phys. Chem. Chem. Phys. **4**, 5613 (2002).
[86]K. M. Hickson, C. M. Sadowski, and I. W. M. Smith, J. Phys. Chem. A **106**, 8442 (2002).
[87]M. H. Alexander, J. Chem. Phys. **99**, 7725 (1993).
[88]P. D. A. Mills, C. M. Western, and B. J. Howard, J. Phys. Chem. **90**, 4961 (1986).
[89]M. H. Alexander, J. Chem. Phys. **111**, 7435 (1999).
[90]Y. Kim, J. Fleniken, H. Meyer, M. H. Alexander, and P. J. Dagdigian, J. Chem. Phys. **113**, 73 (2000).
[91]B. Wen, Y. Kim, H. Meyer, J. Klos, and M. H. Alexander, J. Phys. Chem. A **112**, 9483 (2008).
[92]M. H. Alexander and S. Stolte, J. Chem. Phys. **112**, 8017 (2000).
[93]H. R. Mayne and M. Keil, J. Phys. Chem. **88**, 883 (1984).
[94]A. Degli Esposti, A. Berning, and H.-J. Werner, J. Chem. Phys. **103**, 2067 (1995).
[95]M. C. L. Gerry, A. J. Merer, U. Sassenberg, and T. C. Steimle, J. Chem. Phys. **86**, 4754 (1987).
[96]J. Brown and A. Carrington, *Rotational Spectroscopy of Diatomic Molecules* (Cambridge University Press, Cambridge, England, 2003).
[97]W. L. Meerts and A. Dymanus, J. Mol. Spectrosc. **44**, 320 (1972).